Journal of Fluids and Structures (1994) **8**, 663–680

2-D COMPUTATIONS OF UNSTEADY FLOW PAST A SQUARE CYLINDER WITH THE BALDWIN–LOMAX MODEL

G. B. DENG, J. PIQUET, P. QUEUTEY AND M. VISONNEAU
CFD Group, Laboratoire de Mécanique des Fluides, URA-1217 CNRS
Ecole Centrale de Nantes, 44072, France

(Received 7 September 1993 and in revised form 19 April 1994)

The unsteady turbulent flow past a square cylinder is calculated with the Baldwin–Lomax Model. The influence of the numerical schemes is studied. Comparisons with experimental data and with previous calculations using a Reynolds stress model and 3-D large eddy simulations are presented. It is shown that a good prediction is obtained with a Baldwin–Lomax model by using the recently proposed CPI discretization scheme.

1. INTRODUCTION

HYDRODYNAMIC LOADING ON A CYLINDER-LIKE structure is very important in offshore engineering as well as in many other industrial applications. The most important flow feature in this configuration is the existence of a quasi-periodic vortex-shedding motion in the body wake. This phenomenon has been studied experimentally for a long time—see for instance the reviews by Berger & Wille (1972), King (1977) or Bearman (1984)—but the development of computational facilities makes it possible nowadays to obtain predictions of this type of flow with a high level of detail. Most industrial applications occur in the turbulent regime; hence, turbulence modelling is a key issue for a correct vortex-shedding flow prediction.

Circular and square cylinder cross-sections are most frequently considered in the applications, experimental studies and calculations which have recently been reviewed by Rodi (1992). Experimental observations have identified different flow regimes in the case of a circular cylinder. In the front part of the cylinder, a laminar (but not always steady) stagnation flow region is present. Along the cylinder side wall, flow separation and possible reattachment can be observed. Since the pressure field changes rapidly near the separation and reattachment points, its prediction is decisive for a correct estimation of the drag and lift coefficients. Unfortunately, none of the existing turbulence models seems to be able to describe the pressure field correctly. Also, turbulent flows in an unsteady separation region are not well understood; moreover, they are usually influenced by transition to turbulence. Separated flows are convected downstream into the wake of the cylinder, forming an unsteady vortex street. The flow becomes fully turbulent and is dominated by the mechanism of turbulent convection and dissipation.

An analysis of Cantwell & Coles' (1983) experimental data allowed Franke *et al.* (1989) to show that a region occurs in the wake where the eddy viscosity becomes negative. This fact may explain that predictions with a K-ε type model were unsatisfactory (Franke *et al.* 1989; Franke & Rodi 1991). Direct simulation of turbulent vortex-shedding flow is still unfeasible at present. Ishii *et al.* (1985) have performed a 2-D calculation around a circular cylinder in the supercritical regime using a

0889-9746/94/070663 + 18 $08.00

third-order upwind scheme without any turbulence model; they have claimed that the drag coefficient crisis can be predicted. However, later calculations by Tamura *et al.* (1990) using a similar approach seem to indicate that the apparently successful prediction of the drag crisis is a simple artifact due to the use of a coarse grid, rather than a faithful numerical result. They confirmed, however, that a third-order scheme can be applied to vortex-shedding flow simulation, but that a 3-D calculation is necessary to ensure a successful prediction. Franke & Rodi (1991) have chosen another alternative by using conventional turbulence models. Both the K-ε model and Reynolds-Stress Equations (RSE) have been tested. Results obtained by various versions were analysed by comparing with Lyn's (1992) experimental data around a square cylinder at Re = 22,000. The K-ε based eddy-viscosity models were found to be inadequate to simulate the vortex-shedding flow, while the RSE model gave much better results in terms of global parameters, such as global loads, as well as more detailed quantities such as the total fluctuation energy, in spite of still existing shortcomings.

In our experience, the Baldwin–Lomax (1978) model (hereafter referred to as the BL Model) usually gives better results than a K-ε model in predicting the flow around a body where the pressure gradient is a dominant factor and where several flow regimes exist. In the following, we apply the BL model together with a newly proposed discretization scheme, namely the Consistent Physical Interpolation scheme—hereafter called the CPI scheme for short—(Deng *et al.* 1992) to calculate vortex-shedding flows. It will be shown that a simple algebraic eddy-viscosity model can be rather successful in predicting several significant features of a complex vortex-shedding flow. Results obtained for the square cylinder case will be presented in this paper and compared with available experimental data as well as with previous calculations.

2. GOVERNING EQUATIONS AND TURBULENCE MODEL

The vortex-shedding flows are calculated by solving the two-dimensional ensemble-averaged Navier–Stokes equations,

$$\frac{\partial u_i}{\partial x_i} = 0, \qquad \frac{\partial u_i}{\partial t} + u_j \frac{\partial u_i}{\partial x_j} = -\frac{1}{\rho}\frac{\partial p}{\partial x_i} + \frac{\partial}{\partial x_j}\left[-\overline{u_i' u_j'} + \nu \frac{\partial u_i}{\partial x_j}\right], \tag{1}$$

where the Reynolds stresses are modelled by an eddy-viscosity model,

$$-\overline{u_i' u_j'} = \nu_t\left(\frac{\partial u_i}{\partial x_j} + \frac{\partial u_j}{\partial x_i}\right) - \frac{2}{3}K\delta_{ij}. \tag{2}$$

The eddy viscosity, ν_t, is given by the BL model, while the K-contribution in equation (2) is simply neglected. Momentum equations are solved down to the wall without using a wall function approach. The ensemble-averaged velocity field, u_i, is two-dimensional and its components are denoted hereafter by $\bar{U}$, the x-component which is parallel to the freestream V_∞, and $\bar{V}$, the y-component which is orthogonal to the freestream. For the sake of conciseness, details regarding the BL model are omitted here [see Baldwin & Lomax (1978)]. The distance to the wall, required in the model, is taken as the curvilinear absciss along the "radial" grid lines $\xi = \text{const.}$, with no particular measure in the wake or for transition. Due to the convexity of the geometry and to the O-type grid used in the present calculation, this definition leaves no place for ambiguity in the definition of the length scale.

3. NUMERICAL APPROACH

The unsteady ensemble-averaged Navier–Stokes equations are solved implicitly to avoid a time step restriction. A three-level backward Euler second-order scheme is used:

$$\frac{\partial u_i^{(n)}}{\partial x_i} = 0, \tag{3}$$

$$\frac{3u_i^{(n)} - 4u_i^{(n-1)} + u_i^{(n-2)}}{2\,\Delta t} + \hat{u}_j^{(n)} \frac{\partial u_i^{(n)}}{\partial x_j} = -\frac{1}{\rho}\frac{\partial p^{(n)}}{\partial x_i} + \frac{\partial}{\partial x_j}\left[-\overline{u_i' u_j'^{(n)}} + \nu \frac{\partial u_i^{(n)}}{\partial x_j}\right]. \tag{4}$$

Two kinds of spatial discretization schemes have been tested, namely the UNIEXP scheme (Deng & Piquet 1992) and the CPI scheme (Deng *et al.* 1992). The former is a skew-upwinding scheme based on exponential discretization and is similar to a hybrid scheme; the latter is a finite volume scheme based on a physical interpolation approach recently proposed by the authors: it ensures a second-order accuracy and numerical stability, while keeping a compact nine-point stencil in two-dimensional problems. Another important feature of the CPI scheme is that it ensures both mass and momentum conservation on the same control volumes. The linearized system is solved either with the (segregated) PISO method (Issa 1985) or with a fully coupled method using a Bi-CGSTAB solver (Van der Vorst 1992) with ILU-type preconditionning techniques (Deng *et al.* 1991). The convection velocity, $\hat{u}_j^{(n)}$, is either updated iteratively when the PISO algorithm is used, or extrapolated in time when the fully coupled approach is used, since the linearized algebraic system is solved only once for a given time step. An additional fictitious time step is added to ensure the convergence of the PISO method at each real time step. For each real time step, residuals are reduced by three orders of magnitude for PISO and four orders for Bi-CGSTAB. The Bi-CGSTAB-based fully coupled approach is about five times faster than the (uncoupled) PISO algorithm. Results obtained are nearly identical despite the time extrapolation for $\hat{u}_j^{(n)}$. A typical calculation per cycle on a grid containing about 10,000 points with more than 150 times steps takes about 10 minutes CPU time on the VP200 machine for the PISO algorithm.

4. NUMERICAL RESULTS

Computations have been performed for the case where $\mathrm{Re} = 22{,}000$ for which detailed experimental data are available (Lyn 1992). Franke & Rodi (1991) have used a K-ε model as well as a Reynolds-stress equation model (RSE, hereafter) either with a wall-function approach or with a two-layer approach, on a 186×156 grid. Kato & Launder (1993) have used a K-ε model with wall functions, on a (too coarse) 34×34 grid and on a 104×70 grid with a modified turbulent energy production term. Only their results with the finest grid will be considered in the following. Tamura *et al.* (1990) have used a direct numerical simulation (no turbulence model) also at $\mathrm{Re} = 10^4$ with a 400×100 2-D grid and a $200 \times 100 \times 50$ 3-D grid. Murakami *et al.* (1992) have used a large eddy simulation (LES) on a $99 \times 63 \times 10$ grid at $\mathrm{Re} = 10^5$, the first grid point being located at $0{\cdot}022D$ from the wall. The present calculations use a 121×94 O-type grid (Figure 1), with the first grid point located at $0{\cdot}0015D$ from the wall. The computational domain is extended to $60D$ where $U = 1$, $V = 0$ are imposed as

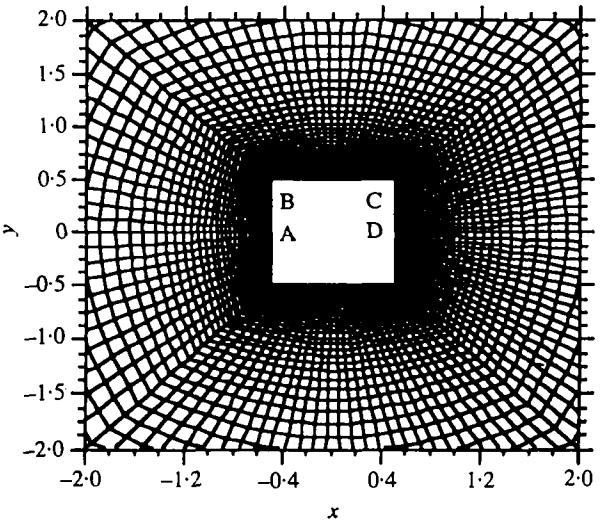

Figure 1. 121 × 94 O-type grid.

boundary conditions; hence the blockage effect is not considered in the present computation. Three calculations have been performed on this working grid (called the coarse grid): the first one uses the UNIEXP scheme with the BL model (UNIEXP-BL model hereafter); the second one uses the CPI scheme with the BL model (CPI-BL model hereafter). In both cases, the BL model is applied everywhere. The third calculation uses the CPI scheme without any turbulence model (hereafter, the CPI model). In the three calculations, the time step used is 0·05. Unlike a large-eddy simulation where only grid-unresolved scales are modelled, stochastic motions are completely modelled in the present calculations with the BL model. With LES, motions of a scale larger than the grid are computed so that, when the grid resolution is increased enough, the simulation tends to become direct. If a conventional model (BL, K-ε, RSE) is used, then, with grid refinement, converged resulting quasi-periodic results are expected to approximate the phase-averaged experimental data.

To check the numerical solution as well as to try to evaluate numerical errors, additional calculations—the so-called fine-grid calculations—have been performed on a 200 × 152 O-type fine grid with the CPI-BL and the UNIEXP-BL model. In the case of the UNIEXP scheme, the linear system arising from the discrete solution of the momentum and of the continuity equations has been solved using a fully coupled technique. The CPI scheme has been solved by the seggregated (PISO) technique since the fully coupled technique has not been implemented in this case. Consequently, the corresponding fine-grid CPI-BL results might be characterized by a slightly insufficient resolution of the divergence-free constraint. Also, another calculation with the UNIEXP-BL model has been performed on a 159 × 140 orthogonal cartesian grid. While the physical domain extends to $60D$ with the O-type fine grid with the same boundary conditions as in the coarser O-grid case, it is defined by the rectangle $-10 \leq x/D \leq 60$; $-7 \leq y/D \leq 7$ on the Cartesian grid, with a periodicity condition along $y/D = \pm 7$ to simulate the blockage effect.

Computational results will be compared both for mean time-averaged and phase-averaged values. Phase-averaging is processed in the same way as in the measurements of Lyn (1992). A pressure signal at the middle of the side-wall ($x = 0$, $y = 0{\cdot}5D$) is recorded. Based on this signal, the shedding cycle, with the frequency f_s, is determined

using a peak-finding algorithm. A phase definition based on peaks was chosen as being more immune to noise and drift. Each cycle thus defined is then divided into 20 equal-sized intervals. Mean time-averaged values over each interval give the phase-averaged value $\bar{u}_{pi}$, $\bar{v}_{pi}$ ($i = 1, 2, \ldots, 20$). It was not found necessary to discard velocity data within the local periods that would be too large (say $>2/f_s$) or too small (say $<0{\cdot}5/f_s$). Although the averaging process is the same, a direct comparison of numerical phase-averaged results with experimental data is not possible, because of a possible phase shift resulting from a low-pass filtering of pressure signals. In the following comparisons, the numerical results are shifted five phases backwards before comparing with the experimental data of Lyn (1992).

The influence of discretization schemes will be seen in the following from a comparison of results obtained with the UNIEXP-BL and CPI-BL model which share in common the use of the BL model and differ only by the numerical scheme used. For a given scheme, the influence of the grid will be seen from a comparison between coarse-grid and fine-grid results. Finally, a comparison between the CPI-BL model and the CPI-model will indicate places where the mean turbulent transport is significant.

Table 1 gathers available experimental data of Lyn (1992), Bearman & Obasaju (1982), Durão *et al.* (1988), Lee (1975), Nakamura & Mizota (1975), Okajima (1982), Otsuki *et al.* (1978), Pocha (1971), Vickery (1966) and Wilkinson (1974) [in Table 1(a)] and computational data of Rodi (1992), Franke & Rodi (1991), Tamura *et al.* (1985), Murakami *et al.* (1992) and Kato & Launder (1993) [in Table 1(b)] relevant to the flow past a square cylinder. From the left to the right of Tables 1(a) and 1(b), we may read the authors, the Reynolds number range for which the data are obtained, the Strouhal number, the maximum and minimum level of the pressure coefficient, $\bar{C}_p$, along the side wall BC, the values of $\bar{C}_p$ at points C and D (see Figure 1)—$\bar{C}_p$(D) being called hereafter the base pressure—the mean drag coefficient, $\bar{C}_D$, the fluctuating drag and lift coefficients, $\tilde{C}_D$ and $\tilde{C}_L$, defined as the amplitude of the main (Strouhal) mode of the lift and drag coefficients resulting from a Fourier analysis—data omitted in Table 1(a) since they have not been measured. Then, the following are given, for the fluctuating pressure coefficient, $C'_p = p'_{\text{r.m.s.}}/(\frac{1}{2}\rho V_\infty^2)$ (where $p'_{\text{r.m.s.}}$ is the root-mean-square value of the wall pressure fluctuation), its maximum and minimum values along BC, and its values at points C and D. Finally, the values, $C'_D = \text{r.m.s.}\,(C_D - \bar{C}_D)$ and $C'_L = \text{r.m.s.}\,(C_L)$, are presented when available. Table 2 gives some information relevant for some of the most useful experimental data (from left to right: authors, data corrected for blockage, aspect ratio of the cylinder and blockage ratio for the wind tunnel, free-stream turbulence level). Quantities left unspecified in Table 2 are not corrected for blockage.

The wake velocity fluctuates in a fairly sinusoidal wave, which results in a sharp spectral peak at the predominant Strouhal frequency. As indicated by Table 1(b), the computed Strouhal number is found, in general, to be smaller than the value 0·135 found by Lyn (1992). The widely accepted data of Okajima (1982) gives St = 0·13 for $10^4 \leq \text{Re} \leq 2 \times 10^4$. Other data are even smaller than these target values, with the exception of the presumably high value 0·139 found by Durão *et al.* (1988). Results with the Reynolds stress equation models are at 0·136 if a wall function is used and at an overestimated value of 0·159 with a two-layer model. The value obtained with a two-layer K-ε model at St = 0·124 is considered too low by Rodi (1992), the K-ε model with wall functions by Kato & Launder (1993) give St = 0·146–0·147 while that used by Franke & Rodi (1991) was unable to generate periodic vortex shedding. Present calculations with the (coarsest) working grid indicate that while the CPI-BL model yields the closest value to Lyn's data at 0·133, the UNIEXP-BL model yields a strongly

TABLE 1(a)

Integral and local parameters (experimental)

Authors	10^{-4}Re	St	$\bar{C}_{pmax}$	$\bar{C}_{pmin}$	$\bar{C}_p$(C)	$\bar{C}_p$(D)	$\bar{C}_D$	C'_{pmax}	C'_{pmin}	C'_p(C)	C'_p(D)	C'_D	C'_L
Bearman & Obasaju	2–7	0·125				−1·45	2·15				0·127		
Bearman & Trueman	0·6–3·2	0·125	−1·9	−1·7	−1·7	−1·7		0·67	0·4	0·4	0·3		1·3
Durão *et al.*	1·4	0·133											
Lee	17·6	0·122	−1·55	−1·5	−1·45	−1·3	2·05	0·75	0·56	0·5	0·35	0·23	1·22
Nakamura	3·3–13	0·125				−1·64							1·0
Okajima	0·1–2·0	0·139											
Otsuki *et al.*	2–3	0·125				−1·3	2·05						
Pocha	9·1	0·12	−1·4	−1·3	−1·2	−1·35	2·06	0·88	0·6	0·6–0·8	0·43	0·18	1·4
Vickery	4–16	0·12				−1·3		0·9	0·05	0·5			1·32
Wilkinson	1–10							0·6	0·55		0·19		
Lyn	2·2	0·135											

TABLE 1(b)

Integral and local parameters (computational). Notation: w.w.f.: "with wall functions", eg: coarse grid results; fg: fine grid results. FR: Franke & Rodi (1991); KL: Kato & Launder (1993); Metal : Murakami *et al.* (1991)

Authors	10^{-4}Re	St	$\bar{C}_{pmax}$	$\bar{C}_{pmin}$	$\bar{C}_p$(C)	$\bar{C}_p$(D)	$\bar{C}_D$	$\tilde{C}_D$	$\tilde{C}_L$	C'_{pmax}	C'_{pmin}	C'_p(C)	C'_D	C'_L
RSE w.w.f. FR	2·2	0·136	−1·75	−2·1	−1·75	−1·5	2·15	0·383	2·11					
2-layer RSE FR	2·2	0·159	−1·95	−2·1	−2·1	−1·78	2·43	0·079	1·84					
2-layer K-ε FR	2·2	0·124	−1·2	−2	−1·2	−1·0	1·79	0·0	0·323					
K-ε w.w.f. KL	2·2	0·147					1·94		1·36					
LES Metal	2·2	0·132	−1·55	−2·15	−1·55	−1·35	2·10	0·120	1·58	0·68	0·25	0·25	0·2	
UNIEXP-BL:cg	2·2	0·115	−1·35	−1·6	−1·42	−1·43	1·978	0·244	1·965	0·78	0·5	0·5	0·25	0·204	0·978
UNIEXP-BL:fg	2·2	0·12	−1·4	−1·52	−1·5	−1·42	2·09			0·76	0·6	0·6	0·42	0·321	0·888
CPI-BL:cg	2·2	0·133	−1·35	−1·9	−1·5	−1·43	2·242	0·385	1·540	0·95	0·6	0·65	0·42	0·32	0·982
CPI-BL:fg	2·2	0·129	−1·35	−1·95		−1·45	2·11			0·95	0·6	0·65	0·33	0·234	0·94
CPI model	2·2	0·157	−1·45	−1·95	−1·8	−1·97	2·643	0·334	1·390	0·95	0·7	0·85	0·85	0·334	1·130

TABLE 2

Some relevant conditions of published experimental data. Notation: A & V: Allen & Vincenti, NACA Report 782 (1944), correction for $\bar{C}_D$

Authors	Data corrected for blockage	Aspect ratio Blockage ratio	Free-stream turbulence level
Bearman & Obasaju	No correction (but 5% on U_∞ with Maskell)	$17D$; 5·5%	<0·04%
Bearman & Trueman	St, $\bar{C}_D$, $\bar{C}_{pb}$ (Maskell); no estimation	>$28D$; <7·2%	<0·3%
Durão *et al.*	No indication	$6D$	6%
Lee	U_∞(3%), $\bar{C}_D$(7%), $\bar{C}_L$(4%), $\bar{C}_{pb}$(10%): A & V	$40D$; 3·6%	0·5%
Nakamura	No indication	$35D$	?
Vickery	$\bar{C}_D$, $\bar{C}_L$(10%), $\bar{C}_p$, St, C'_L with Maskell	$14D$	10%

underestimated value. A laminar flow calculation with the CPI scheme yields an overestimated value of St with a second nondimensional frequency at 0·051, with high C_D and C_L amplitudes of 1·71 and 0·761, respectively, as compared with the amplitudes of the main mode: $\bar{C}_D = 0{\cdot}334$, $\bar{C}_L = 1{\cdot}39$. Hence, the value found for C'_L, in agreement with Bearman, cannot be considered in this laminar flow calculation, as satisfactory. Some fine grid results are also mentioned in Table 1. The Strouhal values obtained by the UNIEXP-BL and CPI-BL models are then 0·12. Such values which agree with LES results must, however, be treated with caution, since the time window cannot be considered to be large enough to validate secondary frequencies which occur in the signal. Also, it is difficult to compare coarse grid and fine grid results for the CPI scheme, since they have not been obtained with identical convergence criteria for the linear systems.

The pressure distribution along the surface of the cylinder is presented in Figure 2 where it is compared with experimental data of Lee (1975) and of Otsuki *et al.* (1978). As indicated in Table 1, although most of Lee's complete data are obtained at

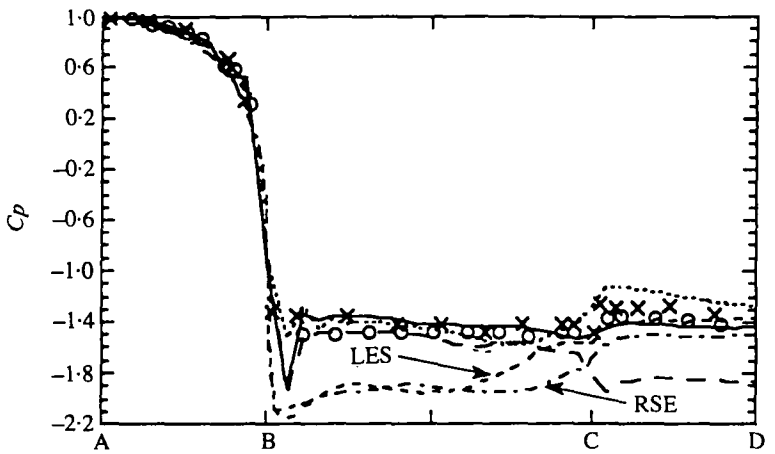

Figure 2. Pressure distribution along the surface of the square cylinder (see Figure 1 for locations of points A, B, C, D). ·····, UNIEXP-BL model; ---, CPI model; —, CPI-BL model; ---, LES model; -·-·-, RSE model; O, Lee (1975) experimental data; ×, Otsuki *et al.* (1978) experimental data.

Reynolds number higher than that for which the calculation is performed, they are similar to other experimental and presently computed ones, as well as Pocha's data (1971). Measurements by Pocha and Otsuki *et al.* share in common a slight decrease of C_p from B to C, a substantial increase close to C, and a continuous decrease of C_p from C to D. Measurements, not corrected for blockage, by Bearman & Obasaju (1982) indicate slightly lower levels of C_p especially along BC and, to a lesser degree, along CD.

The present results using the BL model appear in good agreement with the data of Lee (1975), Otsuki *et al.* (1978) and Pocha (1971). There is a significant effect of the numerical scheme along CD with a 15% variation in C_p, in favour of the CPI scheme (Figure 2). Results on the fine grid look very similar to those obtained on the coarse grid; discrepancies are located mainly close to the edges B and C. It appears also that a laminar calculation using the CPI scheme yields a more negative value and an incorrect decrease of C_p around the edge C. If we now compare the present numerical results with those obtained with the RSE model, we see that the results using a wall function yield substantially lower values of C_p, in agreement with the Bearman & Obasaju results on each side of point C, missing the decreasing trend from C to D. Even lower values, close to $-2{\cdot}0$ along BC and close to $-1{\cdot}8$ along CD, are found with the two-layer RSE model (Rodi 1992). Results of the large eddy simulation indicate a continuous increase of C_p along BC with levels along CD close to $-1{\cdot}4$.

Fluctuating pressures are presented as pressure coefficients, C_p', in Figure 3. The calculations performed in this work are compared with available data of Bearman & Obasaju (1982), Bearman & Trueman (1972) and Pocha (1971). The accuracy of C_p' is rather low (about $\pm 0{\cdot}05$), and, as indicated in Table 1, the scatter between such data is considerable, except along AB. Along BC, data of Bearman & Obasaju (1982), Bearman & Trueman (1972) and Pocha (1971) show a single dominant maximum. Other data show two dominant peaks. These dominant peaks at approximately $D/4$ and $3D/4$ downstream from the front corner are believed to be caused by the movement of the points of separation and reattachment of a separation bubble on the side face beneath the shear layer. While the maximum value of the peaks are similar to those of Pocha and Bearman *et al.*, minimal values of C_p' over CD are far more scattered. Although experimental data exhibit a monotonic decrease of C_p' from C to D, the important scatter along CD is indicated by the base pressures which vary

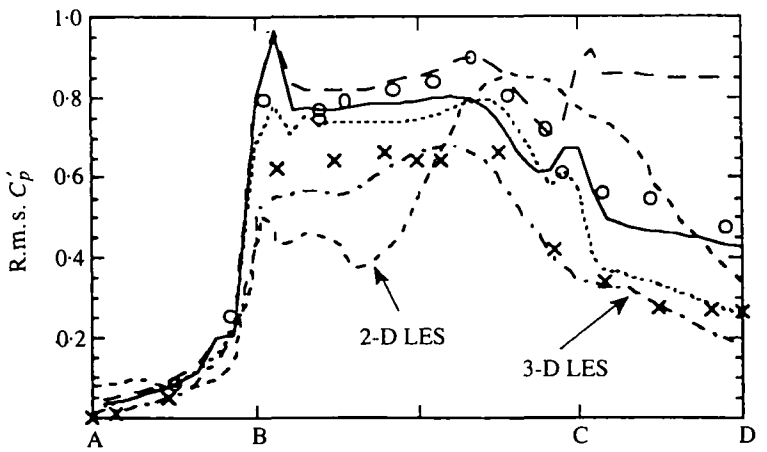

Figure 3. R.M.S. pressure distribution along the surface of square cylinder (same key as Figure 2). O, Pocha (1971), $Re = 9{\cdot}2 \times 10^4$; ×, Bearman & Trueman (1972), $Re = 2{\cdot}0 \times 10^4$.

between $-1{\cdot}3$ and $-1{\cdot}7$. The important variations in C_p' have been attributed to Reynolds number differences (Bearman & Obasaju 1982), at least for the side CD, but present data gathered in Table 1(a) do not support this conclusion. More plausible sources of discrepancy lie in the different aspect ratios (in the spanwise direction) and in the different turbulence levels of the wind tunnel used. Finally, while data of Bearman & Obasaju (1982), Pocha (1971) and Vickery (1966) are free of or corrected for blockage, data of Lee (1975) and Lyn (1992) are not.

Here again, calculations performed with the CPI-BL model yield predictions in good agreement with Pocha's data (1971). It is observed that the laminar-type calculation with the CPI scheme yields also a correct level along BC. However, the base value $C_p'(\mathrm{D})$, about $0{\cdot}85$, is too high and does not decrease towards D. The UNIEXP-BL model again does not perform as well as the CPI-BL model, with $C_p'(\mathrm{D}) = 0{\cdot}27$, in agreement, however, with Bearman & Obasaju (1982). Both models show a very low grid effect, as indicated by significant values of C_p' gathered in Table 1(b). If we now consider large eddy simulations of Murakami *et al.* (1991), it appears that, where the two-dimensional calculation does not fit the trends of experimental data, the three-dimensional calculation is in correct agreement with the data of Bearman & Obasaju (1982), in spite of a low base pressure. The global behaviour of the LES results is similar to, but with a lower level than, our CPI-BL results.

The mean drag coefficient, $\bar{C}_D$, nondimensionalized with the length BC is determined by integrating the mean pressure distribution. Because of significant pressure variations along BD, different values of $\bar{C}_D$ are reported between $2{\cdot}05$ and $2{\cdot}23$ (Rodi 1992). As indicated also by Table 1, the LES and RSE models with wall functions yield a correct agreement with data. The CPI-BL model gives also an acceptable result. In contrast, the two-layer RSE model and the laminar flow calculation with the CPI scheme (CPI model) yield too high a value of $\bar{C}_D$, while the UNIEXP-BL model and the two layer K-ε model of Franke & Rodi (1991) yield a substantially too low values. The K-ε model of Kato & Launder (1993) seems in contrast to yield a correct value. Present results confirm that low values of the drag coefficient occur simultaneously with a high value of the base pressure. The values of the drag and of the Strouhal number obtained have been correlated with the base pressure value. According to Bearman (1984), St $\bar{C}_D$ is well correlated with a linear function of $\kappa = \sqrt{1 - C_{pb}}$ where the base pressure is taken as $C_p(D)$. Although Figure 4 confirms the validty of the correlation, it does not allow a critical appraisal of calculations and rather indicates that errors in C_p along BD balance each other to a certain extent.

Figure 5 displays the calculated time-mean velocity along the centerline with corresponding measurements of Lyn (1992). The best overall agreement with experimental data is obtained again with the CPI-BL model on the fine grid. Close to the cylinder, the time-mean recirculation which shows negative experimental values of $\bar{u}/V_\infty$ close to $-0{\cdot}25$ (Lyn 1992; Durão *et al.* 1988). Where the UNIEXP-BL model yields values around $-0{\cdot}20$, both on the O-type fine grid and on the Cartesian grid, the CPI-BL model yields a minimum about $-0{\cdot}28$ on the coarse grid and of $-0{\cdot}23$ on the fine grid [Figure 5(a)]. Results by other authors systematically underpredict the time-mean recirculation. LES and UNIEXP-BL model peak about $-0{\cdot}1$ while RSE models yield about $-0{\cdot}07$. Results of Kato & Launder (1993) either underpredict the mean value or shift it outward by more than 60%.

The length of the recirculation zone, about $0{\cdot}9$, is correctly predicted using the CPI-BL model which yields about 1, while LES predictions give about $0{\cdot}8$, like the UNIEXP-BL fine grid results [Figure 5(b)]. The laminar flow calculation using the cpi scheme (CPI model), the UNIEXP-BL and the RSE models underpredict

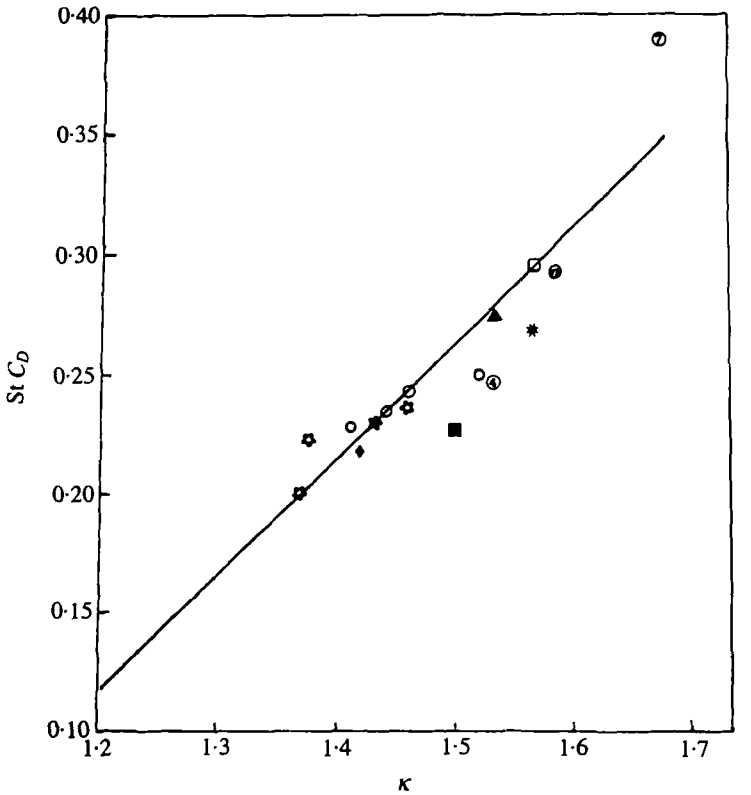

Figure 4. St C_D versus κ for various experiments and calculations. —, Bearman's correlation; ❼, RSE model with wall functions, Franke & Rodi (1991); ⑦, two-layer RSE model, Franke & Rodi (1991); ◆, two-layer K-ε model, Franke & Rodi (1991); ▲, 3D-LES, Murakani *et al.* (1991); □, CPI-BL model; ■, UNIEXP-BL model; ✱, Bearman and Trueman (1972); ✿, collected other Bearman data; ○, Lee data (1975); ④, Pocha data (1971).

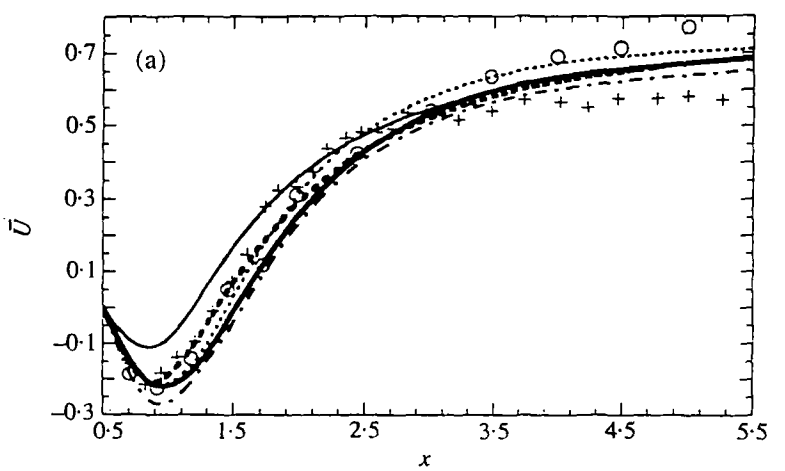

Figure 5(a). Time-averaged mean U-velocity along the centerline. —, UNIEXP-BL model, coarse-grid calculations; ----, UNIEXP-BL model, fine-grid calculations; ····, UNIEXP-BL model, Cartesian grid calculations; ·····, CPI-BL model, coarse-grid calculations; —, CPI-BL model, fine-grid calculations; +, experimental data of Lyn (1992); ○, experimental data of Durão *et al.* (1988).

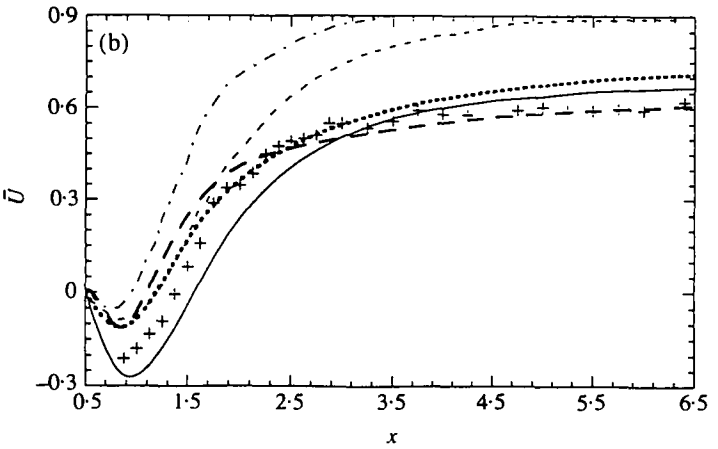

Figure 5(b). Time-averaged mean U-velocity along the centreline. ----- UNIEXP-BL model, fine-grid calculations: —, CPI-BL model, fine-grid calculations; – – –, CPI-model (laminar), coarse-grid calculations; -·-·-, LES calculations of Murakami *et al.* (1992); ·····, RSE calculations of Franke & Rodi (1991), + experimental data of Lyn (1992).

experimental data by about 50%. The UNIEXP-BL model yields results which depend more on the grid used than the CPI-BL model which slightly overpredicts it, especially on the coarse grid [Figure 5(a)]. While the two-layer K-ε model overpredicts the separation length by more than 100%, the K-ε model with wall functions of Kato & Launder (1993) either underpredicts the length of the recirculation together with its intensity or overpredicts it, as already mentioned, by more than 60%. While the two-layer K-ε model underpredicts momentum exchanges resulting from overpredicted periodic fluctuations, the deficiency of RSE models is hardly attributable to the grid used and deserves more investigation.

Further downstream, the best approach to the freestream value is again given by present models. Figure 5(a) shows that the grid effect is small in the recovery region: the level predicted by the CPI-BL and the UNIEXP-BL models is about 10% too high, with a correct trend. The laminar-flow calculation performs almost equally well, indicating a low influence of the turbulent viscosity in the wake. Also, the recovery obtained on a Cartesian grid with the UNIEXP-BL model is identical with that obtained with curvilinear grids, with the same far field behavior. In contrast K-ε, RSE, models and LES results predict a decay of the velocity defect which is dramatically too strong with respect to experimental data of Durão *et al.* (1988) and Lyn (1992) and is presumably due either to the coarse grid used or to the smaller computational domain [Figure 5(b)]. The reasons for which data of Durão *et al.* (1988) depart significantly from those of Lyn (1992) in the far wake are not clear and cannot be fully attributable to the smaller Reynolds number.

Figure 6 presents the distribution of the periodic fluctuation energy along the centerline, as defined by

$$\tilde{K} = \tfrac{1}{20} \sum_{i=1}^{i=20} \tfrac{1}{2}[(\bar{U} - \bar{u}_{pi})^2 + (\bar{V} - \bar{v}_{pi})^2], \tag{5}$$

Experimental points are reconstructed from Lyn's data (1992). The best agreement with experiments is found with the CPI-BL model. This result, which appears only very slightly grid-dependent, is fully consistent with what was found in Figure 5. The UNIEXP-BL model slightly underpredicts the level of $\tilde{K}$. Closer to the rear wall, for

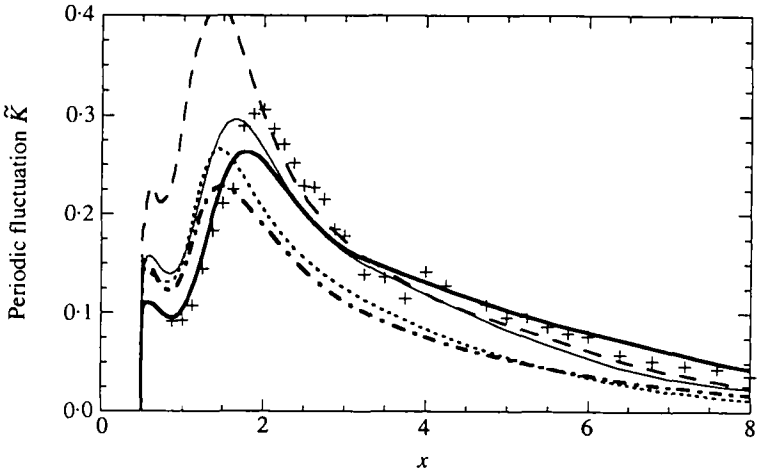

Figure 6. Periodic fluctuation energy along the centerline. ·····, UNIEXP-BL model, coarse-grid calculations; ·-·-·-, UNIEXP-BL model, fine-grid calculations; —, CPI-BL model, coarse-grid calculations; —, CPI-BL model, fine-grid calculations; ----, CPI model (laminar), coarse-grid calculations; +, experimental data of Lyn (1992).

$x < 2$, the laminar flow calculation with the CPI scheme (CPI model) severely overpredicts $\tilde{K}$, more than calculations with the BL model. The good agreement with data of the CPI-BL model, which is improved on the fine grid, is particularly noteworthy. It is tempting to compare the present results with other available experiments. Durão *et al.* (1988) have estimated the total fluctuation energy (periodic + turbulent) along the centerline and they have found that it peaks at about 0·85 for $x = 1{\cdot}7$. The maximum is located as for Lyn's data (1992) which peak at 0·66. As indicated also by Lyn, the mean-time turbulent kinetic energy peaks at 0·32 for $x = 1{\cdot}6$. Detailed calculations have been performed by Franke & Rodi (1991) who found that the RSE model with wall functions yields the best agreement with Lyn's data (1992) for the total fluctuation energy, with a maximum at 0·66 located for $x = 1{\cdot}6$, as compared with the two-layer RSE model (maximum of 0·8 at $x = 1{\cdot}5$) or with the K-ε model (maximum about 0·15 for $x \approx 4{\cdot}5$–5). However, taking into account the mean-time turbulent kinetic energy which peaks about 0·05 for the RSE model with wall functions, it is found that the corresponding periodic fluctuation energy peaks at about 0·6. The maximum is found even higher at about 0·8 for $x = 1{\cdot}5$ with the two-layer RSE model. Therefore, results of Franke & Rodi (1991) using a RSE model severely overpredict the periodic fluctuation energy and underpredict the time-mean turbulent kinetic energy. The two-layer K-ε model yields a very low level of total fluctuation energy (<0·15), and this is also found to a lesser degree with the Kato & Launder (1993) model, using wall functions. Since the time-mean turbulent kinetic energy remains lower than 0·08, the periodic fluctuation energy is also dramatically low. The LES calculation produces also a correct distribution of the total fluctuation energy but the level is underestimated by a factor of two, while the turbulent fluctuation level is also too low in the same amount.

Figure 7 presents the time-averaged $\bar{U}$-velocity at $x = 0$. The influence of the turbulent model is very weak since CPI-BL and CPI models yield similar results; also the CPI scheme appears slightly better than the UNIEXP scheme. However, results are not free from numerical diffusion since the maximum of the (overshooting) velocity profile is slightly damped and shifted away from the wall. It is apparent that the

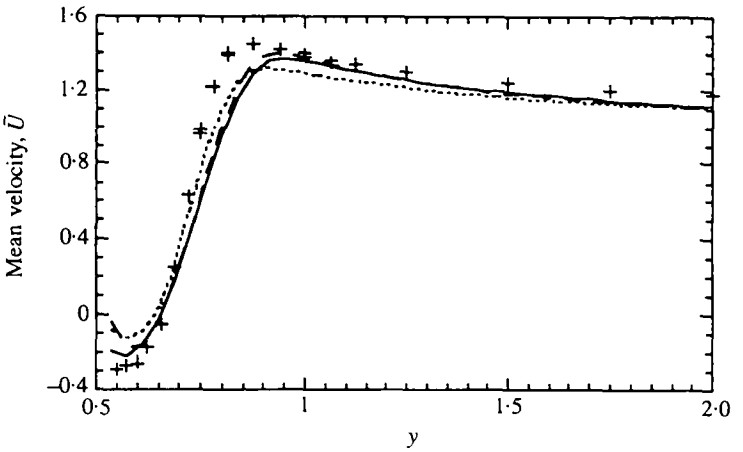

Figure 7. Time-averaged mean U velocity at the middle of the cylinder ($x = 0$). ····, UNIEXP-BL model; —, CPI-BL model; ---, CPI model; +, Lyn's (1992) experimental data.

separation zone is best described by the CPI-BL model, although the intensity of the recirculation is underestimated.

The periodic fluctuation energy is presented in Figure 8 which indicates that maxima are overpredicted by the BL model, in spite of an underpredicted mean velocity gradient. In contrast, the CPI model yields an apparently correct maximum level. Both calculations share in common the existence of a local maximum in the recirculation region.

The aforementioned trends are confirmed by results presented in Figures 9 and 10. They indicate, through the lack of recirculation, that a flow reattachment on the edge BC of the cylinder is observed numerically for some phases, while it does not seem present in experiments of Lyn (1992) and in visualizations of Durão *et al.* (1988). Hence, improving the turbulence modelling is necessary in the separation region along the side wall.

Phase-averaged results along the centerline are presented in Figures 11 to 14. The

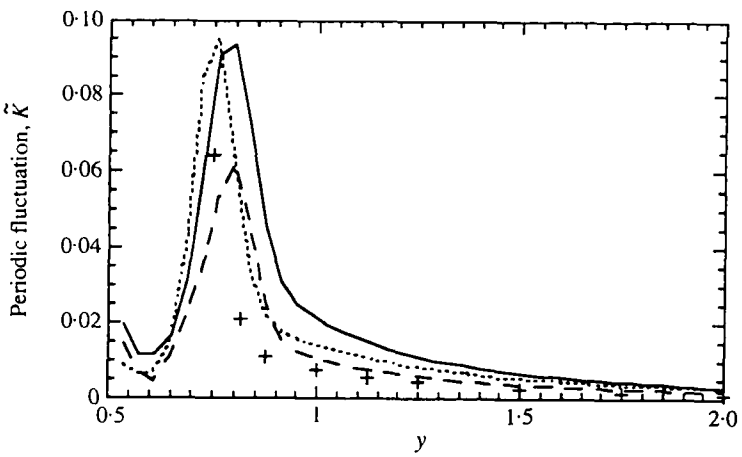

Figure 8. Periodic fluctuation energy at the middle of the cylinder ($x = 0$). ····, UNIEXP-BL model; —, CPI-BL model; ---, CPI model; +, Lyn's (1992) experimental data.

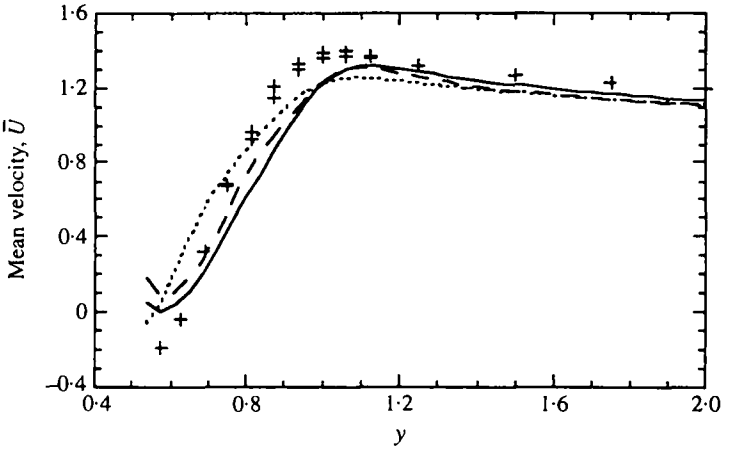

Figure 9. Time-averaged mean U velocity at the edge of the cylinder ($x = 0{\cdot}5$). ····, UNIEXP-BL model; —, CPI-BL model; ---, CPI model; +, Lyn's (1992) experimental data.

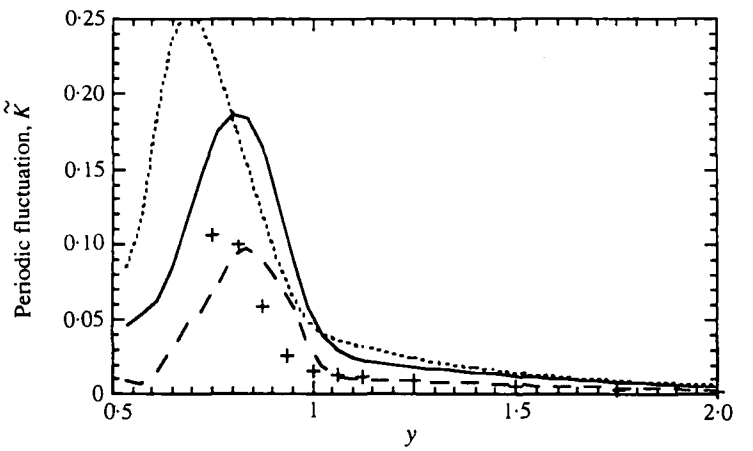

Figure 10. Periodic fluctuation energy at the edge of the cylinder ($x = 0{\cdot}5$). ····, UNIEXP-BL model; —, CPI-BL model; ---, CPI model; +, Lyn's (1992) experimental data.

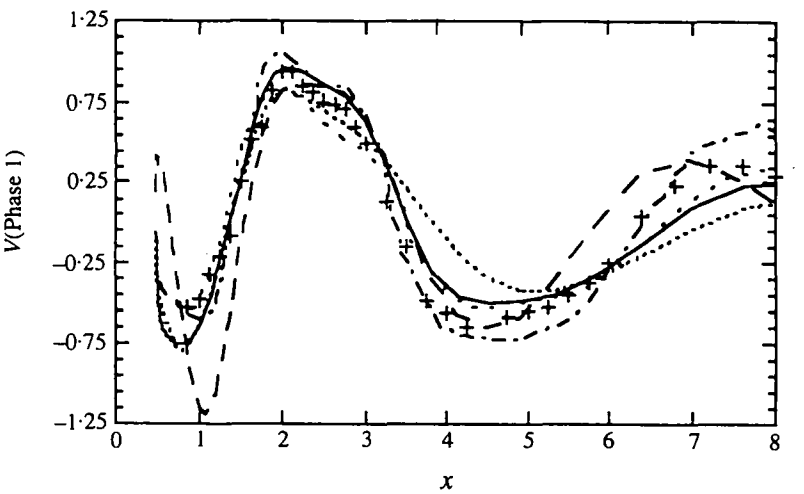

Figure 11. Averaged V-velocity for phase 1 along the centerline. ····, UNIEXP-BL model; —, CPI-BL model; ---, CPI model; -----, RSE model; ····, LES Model; +, Lyn's (1992) experimental data.

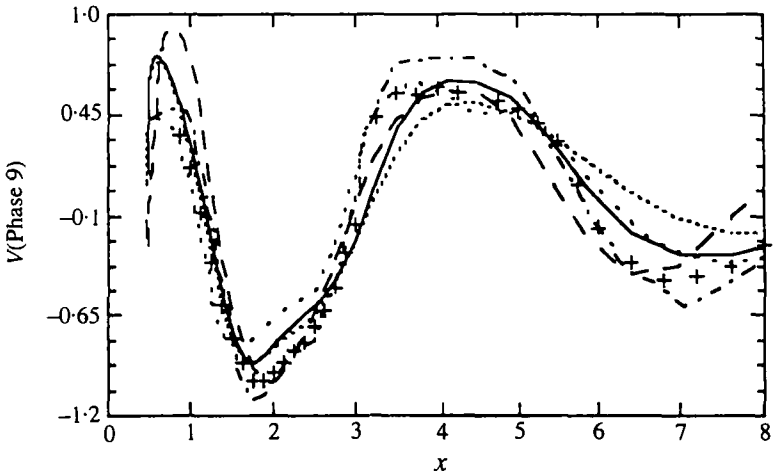

Figure 12. Averaged V-velocity for phase 9 along the centerline. ····, UNIEXP-BL model; —, CPI-BL model; ---, CPI model; -·-·-, RSE model; ····, LES model; +, Lyn's (1992) experimental data.

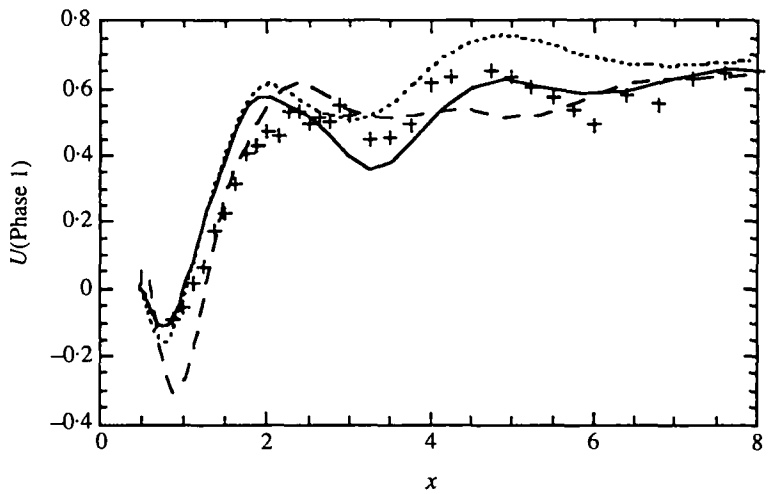

Figure 13. Averaged U-velocity for phase 1 along the centerline. ····, UNIEXP-BL model; —, CPI-BL model; ---, CPI model; +, Lyn's (1992) experimental data.

CPI-BL model is seen again to perform better than the CPI and the UNIEXP-BL models, and at least as well as LES and RSE models (Figures 10 and 11). The vortex street "wave-length" is underpredicted in the laminar flow calculation, and its amplitude seems to be reduced by the BL model.

5. CONCLUSIONS

Vortex-shedding flows have been computed in the past using various eddy-viscosity models. The failure of the K-ε model is mainly due to an unrealistic estimation of the eddy-viscosity in the stagnation region where the flow remains laminar. The BL model has been seen to overcome this difficulty. Successful results have also been reported by Franke & Rodi (1991) with a Reynolds stress equation model. The fact that Murakami

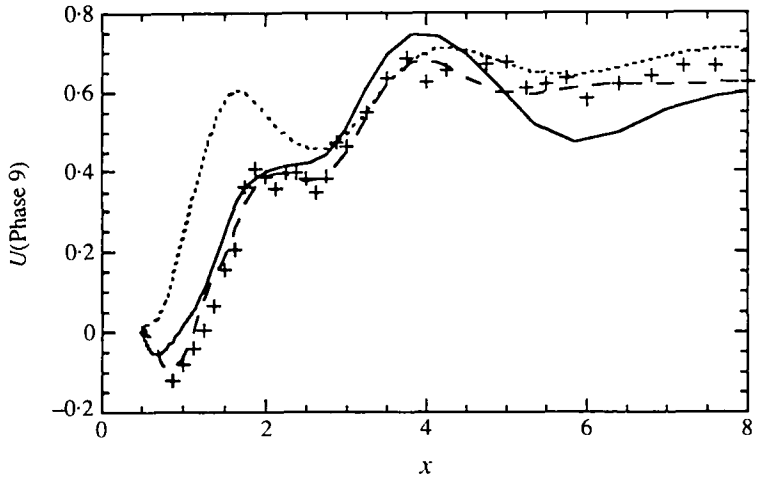

Figure 14. Averaged U-velocity for phase 9 along the centerline. ····, UNIEXP-BL model; —, CPI-BL model; ---, CPI model; +, Lyn's (1992) experimental data.

et al. (1991) and Tamura *et al.* (1990) have also mentioned the unsatisfactory behavior of 2-D LES for vortex-shedding flow simulation deserves special comment.

The flow past a square cylinder is characterized by a great diversity of possible shedding modes which can be distinguished by the flow structure along BC (see Figure 1) and by the shedding wake characteristics, among other phenomena. Usually, depending on physical situations (Re, incidence, blockage, freestream turbulence level, etc.) or on numerical conditions (grid, boundary conditions, turbulence model), one shedding mode, more stable than the others, occurs (a possibility is also that the flow wanders between two competing modes). With a low effective viscosity (or dissipation)—this is presumably the case if no turbulence model is used or if a Smagorinsky model is used—the computed flow is very unstable along BC and eddies are generated [Figure 15(a)]. Increasing the effective viscosity tends to suppress such eddies and to provoke a detachment at point B without reattachment between B and C (Figure 15(b)]. The wake structure will be more complex in the former case than in the latter, resulting in strong cycle-to-cycle variations in the periodic flow pattern. Such a situation has been found with the CPI model (without BL) on the working grid. It is in agreement with the Tamura *et al.* and Murakami *et al.* findings [one can also notice that difficulties encountered by Kao & Launder (1993) are precisely when they diminish the C_μ constant in the K-ε model-see their relation (8)]. If the effective viscosity is increased, using for instance a BL model, the shedding mode becomes more organized

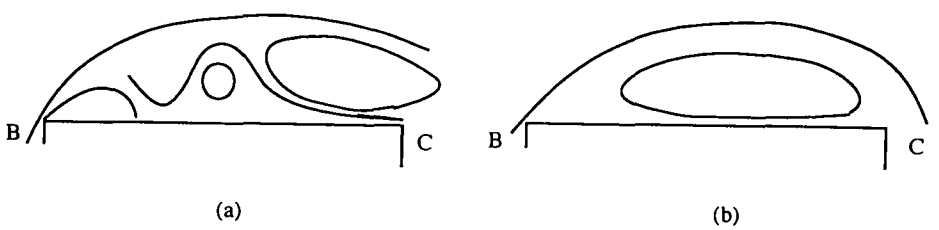

Figure 15. Schematic sketch of instantaneous computed flows along BC: (a) low effective viscosity; (b) high effective viscosity.

with a dominant Strouhal frequency. The fact that Tamura *et al.* (1990) and Murakami *et al.* (1991) call for the use of complete 3-D calculations probably means that the capture of the stable shedding mode is easier in a 3-D calculation, due to the tendency of energy to cascade towards small scales; this would make the disappearance of unstable eddies along BC easier. However, the scarcity of presently available results as well as the technical problems inherent to such methods make it difficult to judge their predictive capabilities.

At least when separation is imposed by a geometric singularity, such as for the square cylinder problem, the present two-dimensional calculations indicate that reasonable results can be expected with a simple algebraic BL model. Turbulence modelling requirements in the recirculation region on the side and behind the cylinder remain, however, unclear. Although none of the existing turbulence models seem to be able to describe the separating boundary layer and the separation region correctly, the BL model yields results which seem even better than a complex RSE model. In the wake, turbulence modelling seems less crucial than near the cylinder, and here, the present model accounts for the weakness of the turbulent stresses correctly. Taken as a whole, such encouraging results do not allow a claim of superiority of the BL model over the RSE Model or the 3-D large eddy simulation for complex vortex-shedding flow predictions, and, even for the square cylinder problem, further examination at higher Reynolds number is needed.

Apart from the turbulence model, it appears also that a full understanding of the discretization scheme is essential. A hybrid skew-upwind type scheme does not seem to be fully adequate, as indicated by results obtained with the UNIEXP-BL model on the coarse grid. The recently proposed CPI scheme looks well suited for high Reynolds number calculations of turbulent flows, especially in the case of a nonuniform grid using a curvilinear coordinate system.

ACKNOWLEDGMENTS

The authors gratefully acknowledge the fruitful correspondence with Professor Rodi and thank Dr Lyn for his unpublished experimental data. Computations have been performed on the VP200 (CIRCE) with CPU time provided by the DS/SPI or CNRS. Partial financial support of DRET through contract 92.046 is also gratefully acknowledged.

REFERENCES

BALDWIN, B. S. & LOMAX, H. 1978 Thin layer approximation and algebraic model for separated flows, AIAA Paper 78-257.

BEARMAN, P. W. 1984 Vortex shedding from oscillating bluff bodies. *Annual Review of Fluid Mechanics* **16,** 195–222.

BEARMAN, P. W. & OBASAJU, E. D. 1982 An experimental study of pressure fluctuations on fixed and oscillating square-section cylinders. *Journal of Fluid Mechanics* **119,** 297–321.

BEARMAN, P. W. & TRUEMAN, D. M. 1972 An investigation of the flow around rectangular cylinders. *Aeronautical Quarterly* **23,** 229–237.

BERGER, E. & WILLIE, R. 1972 Periodic flow phenomena. *Annual Review of Fluid Mechanics* **4,** 313–340.

CANTWELL, B. & COLES, D. 1983 An experimental study of entrainment and transport in the turbulent near wake of a circular cylinder. *Journal of Fluid Mechanics* **136,** 321–374.

DENG, G. B., PIQUET, J., QUEUTEY, P. & VISONNEAU, M. 1992 A fully-implict and fully coupled approach for the simulation of three-dimensional unsteady incompressible flows. *Numerical Simulation of 3D Incompressible Unsteady Viscous Laminar Flows. Numerical Notes in Fluid Mechanics* **36,** 34–45, Vieweg, Braunschweig.

DENG, G. B., PIQUET, J. & VISONNEAU, M. 1991 Viscous flow computations using a fully coupled technique, *Proceedings 2nd Osaka International Colloqium on Viscous Fluid Dynamics in Ship Ocean Technology*, pp. 186–202.

DENG, G. B. & PIQUET, J. 1992 Navier–Stokes computations of horseshoe vortex flows. *International Journal for Numerical Methods in Fluids* **15,** 99–124.

DURÃO, D. F. G., HEITOR, M. V. & PEREIRA, J. C. F. 1988 Measurements of turbulent and periodic flows around a square cross-section cylinder. *Experiments in Fluids* **13,** 298–304.

FRANKE, R., RODI, W. & SCHÖNUNG, B. 1989 Analysis of experimental vortex-shedding data with respect to turbulence modelling. *Proceedings 7th Symposium on Turbulent Shear flows*, paper 24–4, Stanford, CA, U.S.A.

FRANKE, R. & RODI, W. 1991 Calculation of vortex shedding past square cylinder with various turbulence models. *Proceedings 8th Symposium on Turbulent Shear Flows*, paper 20-1, Münich, Germany.

ISHII, K., KUWAHARA, K., OGAWA, S., CHYU, W. J. & KAWAMURA, T. 1985 Computation of flow around a circular cylinder in a supercritical regime. AIAA paper 85–1660.

ISSA, R. I. 1985 Solution of the implicity discretized fluid equations by operator splitting. *Journal of Computational Physics* **62,** 40–65.

KATO, M. & LAUNDER, B. E. 1993 The modelling of turbulent flow around stationary and vibrating square cylinders. ASME Fluids Engineering Conference: Forum on Unsteady Flow (see also UMIST Report TFD/92/13).

KING, R. 1977 A review of vortex shedding research and its application. *Ocean Engineering* **4,** 141–171.

LEE, B. E. 1975 The effect of turbulence on the surface pressure field of a square prism. *Journal of Fluid Mechanics* **69,** 263–282.

LYN, D. A. 1992 Ensemble-averaged measurements in the turbulent near wake of a square cylinder: A guide to the data. Private communication.

MURAKAMI, S., MOCHIDA, A., HAYASHI, Y. & SAKAMOTO, S. 1991 Numerical study on velocity-pressure field and wind forces for bluff bodies with k-ε, ASM and LES. *Proceedings 8th International Conference on Wind Engineering*, London, Ontario, Canada.

NAKAMURA, Y. & MIZOTA, T. 1975 Unsteady lifts and wakes of oscillating rectangular prisms. *ASCE Journal of the Engineering Mechanics Division* **101,** 855–871.

OKAJIMA, A. 1982 Strouhal numbers of rectangular cylinders. *Journal of Fluid Mechanics* **123,** 379–398.

OTSUKI, Y., FUJI, K., WASHIZU, K. & OHAYA, A. 1978 Wind tunnel experiment on aerodynamics forces and pressure distributions of rectangular cylinders in a uniform flow. *Proceedings 5th Symposium on Wind Effects on Structures*, pp. 169–175, Tokyo, Japan.

POCHA, J. J. 1971 On unsteady flow past cylinders of square cross-section. Ph.D. Thesis, Department of Aeronautics, Queen Mary College, London, U.K.

RODI, W. 1992 On the simulation of turbulent flow past bluff bodies. *Proceedings 1st International Symposium on Computational Wind Engineering*, Tokyo, Japan.

TAMURA, T., ICHIRO, O. & KUWAHARA, K. 1990 On the reliability of two-dimensional simulation for unsteady flows around a cylinder-type structure. *Journal of Wind Engineering and Industrial Aerodynamics* **35,** 275–298.

VAN DER VORST, H. 1992 BiCGSTAB: a fast and smoothly converging variant of Bi-CG for the solution of nonsymmetric linear systems, *SIAM Journal of Scientific and Statistical Computing* **13,** 631–644.

VICKERY, B. J. 1966 Fluctuating lift and drag on a long cylinder of square cross-section in a smooth and in a turbulent stream. *Journal of Fluid Mechanics* **25,** 481–494.

WILKINSON, R. H. 1974 On the vortex-induced loading on long bluff cylinders. Ph.D. Thesis, Faculty of Engineering, University of Bristol, England.